

IGM Reionization and 21cm Observations

Benedetta Ciardi^{*†}

Max Planck Institute for Astrophysics

E-mail: ciardi@mpa-garching.mpg.de

With the advent in the near future of radio telescopes as LOFAR, a new window on the high-redshift universe will be opened. In particular, it will be possible, for the first time, to observe the 21cm signal from the diffuse intergalactic medium (IGM) prior to its reionization and thus probe the dark ages. In this talk I have discussed about the theoretical modeling of the reionization process, the observability of the 21cm signal from the diffuse IGM and the efforts ongoing within the LOFAR Epoch of Reionization Working Group.

*International Workshop on Cosmic Structure and Evolution - Cosmology2009,
September 23-25, 2009
Bielefeld, Germany*

^{*}Speaker.

[†]Special thanks to all the collaborators mentioned in my talk.

1. Introduction

After the Big Bang the Universe is filled with hot plasma. Following its expansion though the gas cools down and eventually becomes neutral at $z \sim 1300$ (recombination epoch). The period which follows is commonly known as the Dark Ages and ends when the first structures start to form and produce ionizing radiation. This marks the beginning of the reionization process, which is complete by $z \sim 6$. Eventually, these early structures evolve into those observed presently.

From an observational point of view, information on the Universe at the recombination epoch is available via the detection of the Cosmic Microwave Background (CMB) radiation, while the present generation of telescopes in the UV/optical/IR probe the cosmos up to $z \sim 8$ (e.g. Ota et al. 2007; Ouchi et al. 2009; Salvaterra et al. 2009). Nevertheless a large observational gap still exist, that will be partially covered by the planned generation of instruments that will explore the FIR and radio bands.

Why is the intergalactic medium ionized? Evidence of the reionization of the intergalactic medium (IGM) comes from the observations of high- z quasars, whose spectra show absorption features due to neutral hydrogen intervening between the quasars and the observer. The HI optical depth can be written as:

$$\tau_{HI} \sim 6.5 \times 10^5 x_{HI} \left(\frac{1+z}{10} \right)^{1.5}, \quad (1.1)$$

where x_{HI} is the fraction of HI. Given the extremely high value of τ_{HI} , the fact that we observe radiation at frequencies larger than the Ly α emitted by the quasars indicates that the intervening IGM must be in a highly ionization state and x_{HI} close to zero.

Observational constraints on the reionization process. Because the intensity of the absorption observed in the quasars' spectra depends on the amount of HI present, observations of high- z quasars are used to put constraints on the abundance of neutral hydrogen at high redshift. The value inferred from these observations though can vary substantially, with $x_{HI} > 0.1$, $x_{HI} > 0.033$, $x_{HI} < 0.06$ (e.g. Wyithe & Loeb 2004; Oh & Furlanetto 2005; Mesinger & Haiman 2007; Maselli et al. 2007; Bolton & Haehnelt 2007), just to mention a few.

An additional observational constraint comes from the detection of anisotropies in the power spectrum of the CMB, induced by the interaction between the CMB photons and the electrons produced during the reionization process. More precisely, the value of the Thomson scattering optical depth, τ_e , measured by WMAP after 1, 3 and 5 years of operation is 0.16 ± 0.04 , 0.09 ± 0.03 and 0.087 ± 0.017 respectively (Kogut et al. 2003; Spergel et al. 2007; Dunkley et al. 2008). As $\tau_e \propto \int n_e(z) dz$, where n_e is the electron number density, it gives an estimate of the global amount of electrons produced during the reionization process, but no information is available on how these electrons are distributed in space and time.

Thus, the available observations offer constraints on the latest stages of reionization and on the global amount of electrons produced, but to have information on, e.g., the sources of ionization or the history of the reionization process, different type of observations are needed (see Sec. 3).

Theoretical modeling of the reionization process. The ingredients necessary to describe the reionization process are the following:

- a model to follow the formation and evolution of galaxies, possibly including the various feedback effects that regulate the process;

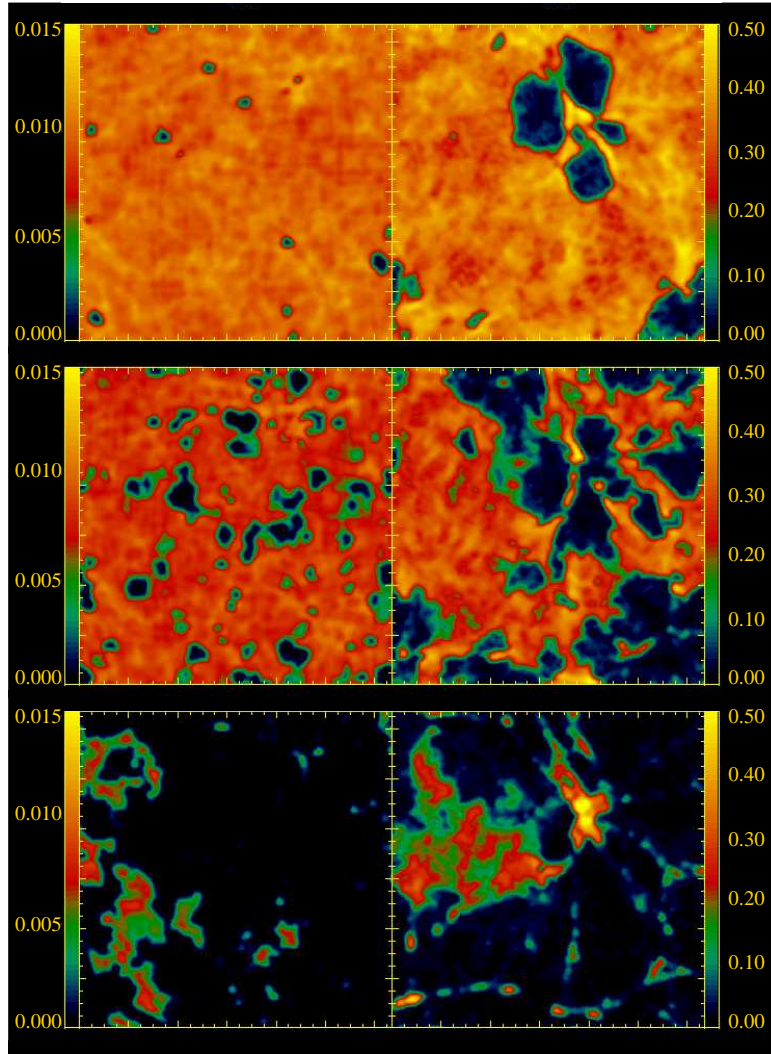


Figure 1: Reionization maps showing the redshift evolution of the number density of neutral hydrogen in the field ($L = 20h^{-1}$ Mpc comoving box; left panels) and in a protocluster environment ($L = 10h^{-1}$ Mpc comoving box; right panels). From top to bottom the redshift of the simulations is 15.5, 12 and 9 (Ciardi, Stoehr & White 2003; Ciardi, Ferrara & White 2003).

- the properties of the ionizing sources, which could be of stellar type, quasars or more exotic sources like e.g. dark matter decay or annihilation;
- a method to follow the propagation of the photons emitted by such sources.

While the second item is probably the most uncertain and parameters (e.g. for stellar type sources their Initial Mass Function [IMF] or the escape fraction of ionizing photons, f_{esc}) are needed to describe the properties of the sources, the third item is the most challenging from a numerical point of view. In fact, the full solution of the seven dimension radiative transfer (RT) equation (three spatial coordinates, two angles, frequency and time) is still well beyond our computational capabilities and, although in some specific cases it is possible to reduce its dimensionality, for the reionization process no spatial symmetry can be invoked. Thus, an increasing effort has been devoted to the de-

velopment of radiative transfer codes based on a variety of approaches and approximations, which have been tested and compared in Iliev et al. (2006).

2. Simulations of cosmic reionization

Through the years our group has run several simulations of IGM reionization (*i*) using simulations of galaxy formation of box dimension 10-20 h^{-1} Mpc comoving run at the MPA (Springel et al. 2000; Stoehr et al. 2004) to retrieve the properties of gas and galaxies; (*ii*) adopting different characteristics for the source properties (i.e. adopting for the stellar sources a standard Salpeter IMF or a Larson IMF biased towards massive stars; varying the value of the escape fraction of ionizing photons in the range 5-20 %); (*iii*) using the Monte Carlo radiative transfer code CRASH (Ciardi et al. 2001; Maselli, Ferrara & Ciardi 2003; Maselli, Ciardi & Kanekar 2009) to follow the propagation of ionizing photons. In some simulations we also included sub-grid physics to take into account the effect of unresolved minihalos on the reionization process. In Figure 1 a typical reionization history is shown (Ciardi, Stoehr & White 2003; Ciardi, Ferrara & White 2003; Ciardi et al. 2006).

The reionization histories mentioned above produce a Thomson scattering optical depth in the range 0.11-0.17, depending on the parameters/approximations adopted. Thus, the uncertainties in the theoretical modeling of the reionization process are still large enough to accommodate the value of τ_e measured by the WMAP satellite (see Introduction). In order to put more severe constraints on our theoretical models a different type of observations is needed.

3. 21cm line diagnostic

The ideal observation to shed light on the reionization process is the detection of the 21cm line from neutral hydrogen (see Furlanetto, Oh & Briggs 2006 for a review on the topic). The ground state of HI has a hyperfine structure and anytime a transition takes place between the hyperfine states a photon is emitted or absorbed with a wavelength of 21cm. Thus, observations at different frequencies would give information on the state of HI at different redshifts, providing insight on the spatial and temporal evolution of the reionization process.

Such a line is expected to be observed in terms of the effects that it has on a background radiation. Typically, the CMB is considered. What we expect to observe is then the differential brightness temperature, δT_b , between the CMB and a patch of HI with optical depth τ_{HI} and spin temperature T_s (which regulates the population of the atomic levels). This is given by:

$$\delta T_b \sim \frac{T_s - T_{CMB}}{1+z} \tau_{HI} \propto \left(1 - \frac{T_{CMB}}{T_s}\right), \quad (3.1)$$

where T_{CMB} is the CMB temperature. From the above equation follows that if T_s is equal to T_{CMB} δT_b is zero and no line can be observed, if instead it is larger (smaller) than T_{CMB} the line is expected to be observed in emission (absorption) against the CMB. Thus, the value of the spin temperature is crucial for the observation of the line. T_s can be written as a weighted mean between T_{CMB} and the kinetic temperature of the gas, T_k :

$$T_s = \frac{T_{CMB} + (y_\alpha + y_c)T_k}{1 + y_\alpha + y_c}, \quad (3.2)$$

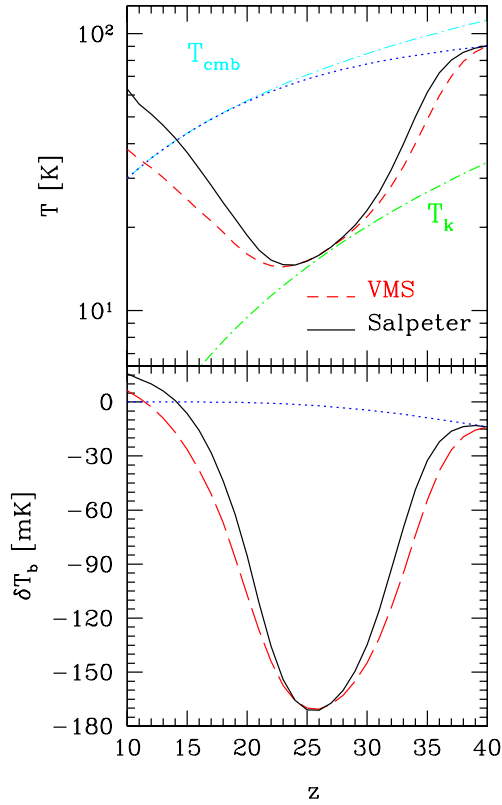


Figure 2: *Upper panel:* Evolution of the spin temperature for a Salpeter (solid lines) and a VMS (dashed) IMF, and in the absence of a $\text{Ly}\alpha$ background (dotted). T_{CMB} and T_k are plotted as upper and lower dotted-dashed lines, respectively. *Lower panel:* Evolution of the differential brightness temperature. Lines are the same as in the upper panel. See Ciardi & Salvaterra (2007) for details.

where y_α and y_c is the efficiency in coupling T_s to T_k due to $\text{Ly}\alpha$ scattering and collisions (with H atoms, electrons and protons) respectively (see Ciardi & Salvaterra 2007 for the values adopted here). While at $z > 20$ y_c is dominant, at lower redshift scattering with the $\text{Ly}\alpha$ photons emitted by the first stars is the most efficient process (Wouthuysen 1952; Field 1959; Hirata 2006; Pritchard & Furlanetto 2006). In addition, $\text{Ly}\alpha$ photons could be able to heat the IGM temperature above the CMB temperature and render the 21cm line visible in emission.

The general picture that we expect is shown in Figure 2 for two different populations of stars producing $\text{Ly}\alpha$ photons, i.e. metal-free stars with a Salpeter IMF and Very Massive Stars (VMS) with a mass of $300 M_\odot$. In the upper panel we show the evolution of the spin temperature for a Salpeter (solid lines) and a VMS (dashed) IMF, and in the absence of a $\text{Ly}\alpha$ background (dotted). T_{CMB} and T_k are plotted as upper and lower dotted-dashed lines, respectively. In the lower panel the evolution of the corresponding differential brightness temperature is shown. At very high redshift $T_s = T_k = T_{\text{CMB}}$ and thus no signal is expected. Once the evolution of T_{CMB} and T_k decouples, collisions in the gas are efficient in maintaining an equilibrium between T_s and T_k and thus the line can be observed in absorption, but at $z < 20$ collisions are not efficient anymore and a thermal equilibrium with the CMB is quickly reached. This is the epoch when the first sources of radiation

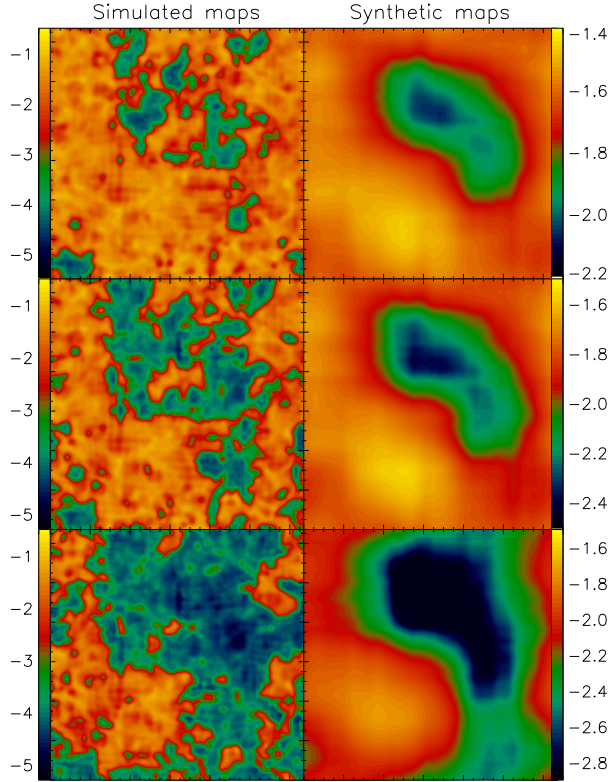


Figure 3: Logarithmic brightness temperature, $\log[\delta T_b/K]$, maps (linear size ≈ 11 arcmin) of the 21cm emission at redshifts $z = 10.6, 9.89, 9.26$ from top to bottom, respectively. Left panels: maps obtained directly from the simulation, i.e. before convolution with LOFAR characteristics; Right: LOFAR synthetic maps. For details see Valdes et al. (2006).

turn on which, in addition to the ionizing photons that initiate the reionization process, emit also Ly α photons. If we assume that they are produced by a population of metal-free stars with either a Salpeter IMF or VMS we find that the 21cm line can actually be observed also in this redshift range, initially in absorption against the CMB, and, once the IGM has been heated above the CMB, in emission. For the case shown in the Figure, the redshift at which the transition between absorption and emission takes place is ~ 15 (12) for a Salpeter IMF (VMS) (for details see Ciardi & Salvaterra 2007).

It should be noticed that the above estimates assume the existence of a Ly α background, although inhomogeneities might be expected. If present, fluctuations in the Ly α background can influence the observability of the line. We are starting to tackle this problem using the radiative transfer code CRASH α (Pierleoni, Maselli, Ciardi 2009) which follows the parallel propagation of both continuum UV photons and the scattering of Ly α photons.

In addition to Ly α photons, other sources of heating can be present in the high redshift universe, as e.g. x-ray photons from an early population of mini-quasars. Using the output of SPH simulations designed to follow the formation of massive black holes at $z \sim 6$ (Pelupessy, Di Matteo

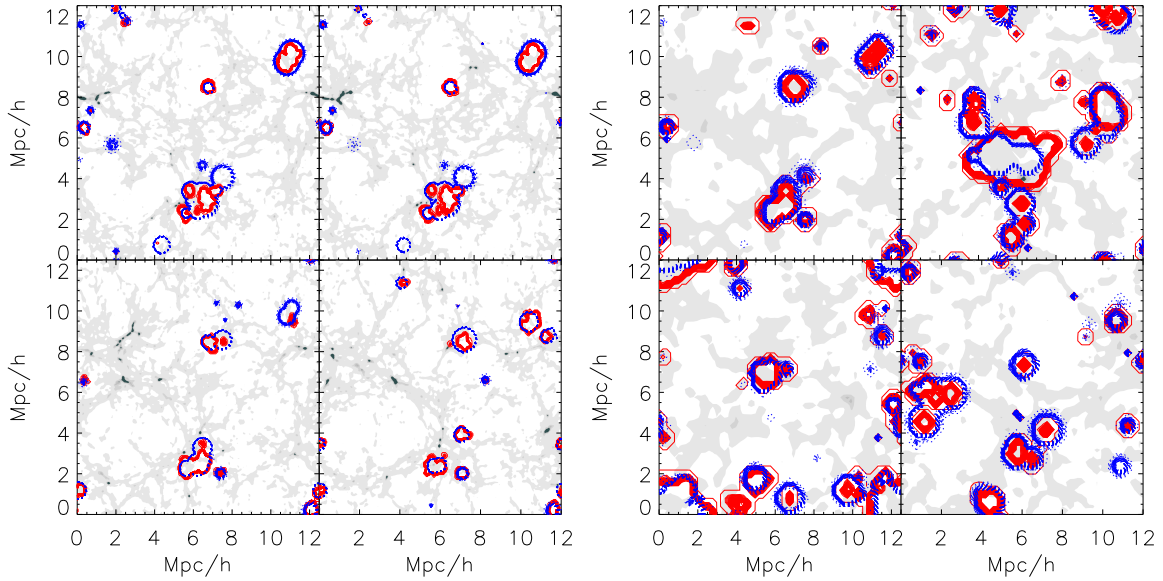


Figure 4: Four slices randomly selected along a direction in the box are plotted that displays the contours (three levels [0, 0.5, 1]) of the neutral fraction of CRASH (red) and BEARS (cyan) at $z = 6$ in 256^6 (left panel) and 64^3 (right panel) grid box of $12 h^{-1}$ Mpc comoving size. The underlying light gray contours represent the dark matter overdensities. See Thomas et al. (2009) for details.

& Ciardi 2007), we have self-consistently estimated the relative contribution to heating from x-rays produced by quasars and $\text{Ly}\alpha$ photons emitted by stellar type sources. We find that, for all the models considered, the x-ray heating is always dominant (Ciardi, Salvaterra & Di Matteo 2009). Nevertheless, also in this case a homogeneous background has been assumed, while a proper radiative transfer of the various components should be followed to assess the exact contribution of UV, x-rays and $\text{Ly}\alpha$ photons to the ionization and heating of the gas.

Once the value of T_s is known, from the distribution of HI provided by simulations of reionization maps of differential brightness temperature can be derived and analyzed to retrieve quantities relevant to observations. Ideally tomography of the IGM will be feasible, allowing to obtain maps of 21cm emission/absorption at different redshift (see Fig. 3). In practice, this will not be achieved during the first few operational years of the present generation of radio telescopes (such as LOFAR or MWA) and instead statistical signatures (e.g. the power spectrum of fluctuations of differential brightness temperature) will be sought after.

4. LOFAR

Among others, the LOFAR telescope is already in a very advanced construction phase and data will start flowing next year. By then, ad hoc theoretical predictions should be available to be compared with observations. To this aim, very large boxes (several hundreds of Mpc) are needed. On these scales the use of fully consistent 3D RT calculations (as the ones mentioned above) is prohibitively expensive and an alternative approach is needed. Within the LOFAR Epoch of Reionization (EoR) Working Group a great effort in this direction is being made. In particular, a method has been developed based on a combination of numerical simulations and the 1D RT code

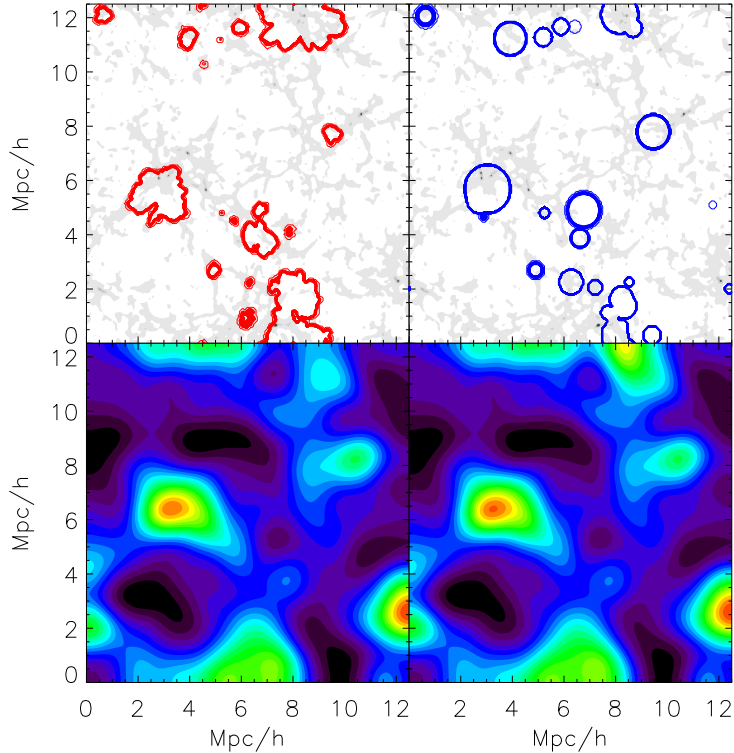


Figure 5: The ionization fronts of CRASH (red contours, top left) and BEARS (blue contours, top right) are overplotted on the underlying density field shown in light grey. This slice is extracted from a 256^3 box at redshift six. The corresponding figures below show the images after being smoothed by the beam response of the antenna. See Thomas et al. (2009) for details.

BEAR (Thomas & Zaroubi 2008). Before applying this method to produce realistic, very large scale reionization histories, its validity needs to be checked against a full RT approach. We have thus compared the performances of CRASH and BEAR on smaller boxes in a variety of test cases (Thomas et al. 2009). In Figure 4 random slices cut through the simulation boxes are shown for different grid sizes at $z = 6$. The lines are isocontours of neutral fraction. Although the details of the reionization structure present some differences due to the inherent spherical symmetry of the 1D approach, the overall agreement is remarkably good, of the order of few percents in terms of average neutral fraction.

What is more important though is that, once the simulations have been convolved with the noise and the beam response of the telescope, the images look almost identical, as can be seen in Figure 5. This means that, for the purposes of modeling the reionization process for LOFAR observations the approximated approach is sufficient.

The final aim is to produce a series of reionization histories associated to the 21cm signal. On top of these, the contribution from both extragalactic and Galactic foregrounds will be added to obtain mock observations as the example shown in Figure 6. The ultimate challenge for the detection of the cosmological signal will be to separate it from the foreground signal, which is orders of magnitude higher. Thus, in addition to simulating mock reionization histories an ongoing effort is being done to identify the best technique to extract the primary signal (e.g. Harker et al.

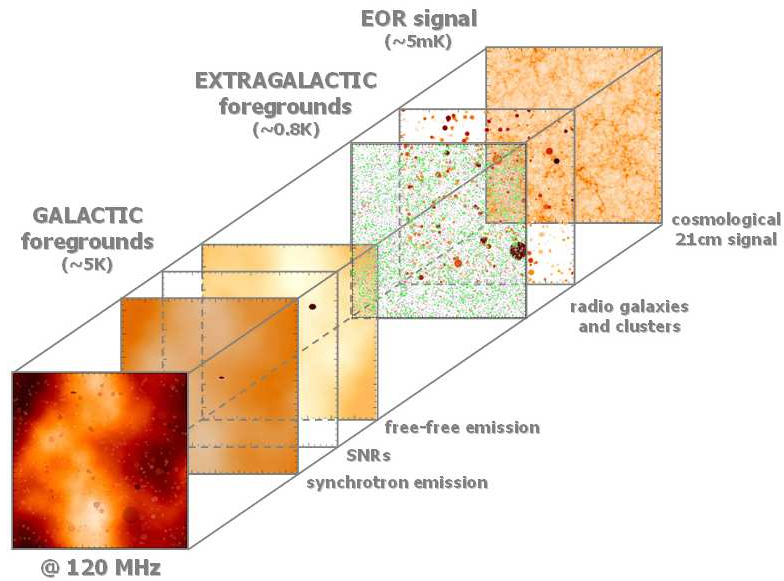


Figure 6: Pipeline showing the building of a mock observation at a nominal frequency of 120 MHz: on top of the cosmological signal, the extragalactic and Galactic foreground contamination is added (Jelic et al. 2008).

2009a, 2009b).

References

- [1] Bolton J. S., Haehnelt M. G., 2007, MNRAS, 374, 493
- [2] Ciardi B., Ferrara A., Marri S., Raimondo G., 2001, MNRAS, 324, 381
- [3] Ciardi B., Scannapieco E., Stoehr F., Ferrara A., Iliev I. T., Shapiro P., 2006, MNRAS, 366, 689
- [4] Ciardi B., Ferrara A., White S.D.M., 2003, MNRAS, 344, L7
- [5] Ciardi B., Salvaterra R., 2007, MNRAS, 381, 1137
- [6] Ciardi B., Salvaterra R., Di Matteo T., 2009, MNRAS, in press, arXiv:0910.1547
- [7] Ciardi B., Stoehr F., White S.D.M., 2003, MNRAS, 343, 110
- [8] Dunkley et al. 2008, astro-ph/0803.0586
- [9] Field G. B., 1959, ApJ, 129, 551
- [10] Furlanetto S. R., Oh S. P., Briggs F. H., 2006, Phys. Rep., 433, 181
- [11] Harker G., et al., 2009a, MNRAS, 393, 1449
- [12] Harker G., et al., 2009b, MNRAS, 397, 1138
- [13] Hirata C. M., 2006, MNRAS, 367, 259

- [14] Iliiev I. T., et al., 2006, MNRAS, 371, 1057
- [15] Jelic V., et al., 2008, MNRAS, 389, 131
- [16] Kogut A., et al. 2003, ApJS, 148, 161
- [17] Maselli A., Ciardi B., Kanekar A., 2009, MNRAS, 393, 171
- [18] Maselli A., Ferrara A., Ciardi B., 2003, MNRAS, 345, 379
- [19] Maselli A., Gallerani S., Ferrara A., Choudhury T. R., 2007, MNRAS, 376, L34
- [20] Mesinger A., Haiman Z., 2007, ApJ, 660, 923
- [21] Oh S. P., Furlanetto S. R., 2005, ApJ, 620, L9
- [22] Ota K., et al., 2007, ApJ, 677, 12
- [23] Ouchi M., et al., 2009, ApJ, 696, 1164
- [24] Pelupessy I., Di Matteo T., Ciardi B., 2007, ApJ, 665, 107
- [25] Pierleoni M., Maselli A., Ciardi B., 2009, MNRAS, 393, 872
- [26] Pritchard J. R., Furlanetto S. R., 2006, MNRAS, 367, 1057
- [27] Salvaterra R., et al., 2009, Nature, 461, 1258
- [28] Spergel D. N., et al. 2007, ApJS, 170, 377
- [29] Springel V. et al. 2000
- [30] Stoher F. et al. 2004
- [31] Thomas R. M., Zaroubi S., 2008, MNRAS, 375, 1269
- [32] Valdes M., Ciardi B., Ferrara A., Johnston-Hollit M., Rottgering H., 2006, MNRAS, 369, L66
- [33] Wouthuysen S. A., 1952, AJ, 57, 31
- [34] Wyithe J. S. B., Loeb A., 2004, Nature, 427, 815